INFECTION AND IMMUNITY, Sept. 2008, p. 3975–3983 Vol. 76, No. 9
0019-9567/08/$08.00+0 doi:10.1128/IAI.00282-08

In Vivo Demonstration and Quantification of Intracellular *Bacillus anthracis* in Lung Epithelial Cells▽

Brooke H. Russell,[1] Qing Liu,[1] Sarah A. Jenkins,[1] Michael J. Tuvim,[2] Burton F. Dickey,[2] and Yi Xu[1]*

Center for Extracellular Matrix Biology, Institute of Biosciences and Technology, Texas A&M Health Science Center, Houston, Texas 77030,[1] and Department of Pulmonary Medicine, University of Texas M. D. Anderson Cancer Center, Houston, Texas 77030[2]

Received 29 February 2008/Returned for modification 2 April 2008/Accepted 24 June 2008

Inhalational anthrax is initiated by the entry of *Bacillus anthracis* spores into the lung. A critical early event in the establishment of an infection is the dissemination of spores from the lung. Using in vitro cell culture assays, we previously demonstrated that *B. anthracis* spores are capable of entering into epithelial cells of the lung and crossing a barrier of lung epithelial cells without apparent disruption of the barrier integrity, suggesting a novel portal for spores to disseminate from the lung. However, in vivo evidence for spore uptake by epithelial cells has been lacking. Here, using a mouse model, we present evidence that *B. anthracis* spores are taken up by lung epithelial cells in vivo soon after spores are delivered into the lung. Immunofluorescence staining of thin sections of lungs from spore-challenged BALB/c mice revealed that spores were associated with the epithelial surfaces in the airway and the alveoli at 2 and 4 h postinoculation. Confocal analysis further indicated that some of the associated spores were surrounded by F-actin, demonstrating intracellular localization. These observations were further confirmed and substantiated by a quantitative method that first isolated lung cells from spore-challenged mice and then stained these cells with antibodies specific for epithelial cells and spores. The results showed that substantial amounts of spores were taken up by lung epithelial cells in vivo. These data, combined with those in our previous reports, provided powerful evidence that the lung epithelia were directly targeted by *B. anthracis* spores at early stages of infection.

Anthrax is caused by the entry of *Bacillus anthracis* spores into the host via the lung, the gastrointestinal tract, or cuts or abrasions on the skin. Among the three forms of anthrax, the inhalational form has the highest fatality rate, approximately 50% even with antibiotic treatment. The initial stage of the infection does not display any distinctive symptoms. As the organism spreads and multiplies in the body, the disease rapidly progresses, resulting in damage to vital organs and eventually death.

Recent inhalational anthrax animal studies suggested that the infection of the lung is most likely secondary, i.e., that after entering into the respiratory system, spores disseminate into the circulation, germinate to become vegetative bacilli, and then infect the lung via the blood (14, 15, 23). Therefore, a crucial step in the establishment of anthrax via the pulmonary route is for the spores to breach the respiratory mucosal barrier. To date, a clear understanding of how this breach is achieved remains to be established.

Three routes have been proposed: alveolar macrophages (17, 18), dendritic cells (DCs) (6, 8), and epithelial cells (31, 32). The macrophage and DC routes are similar in the sense that both macrophages and DCs act as a "Trojan horse," taking up spores from the airway and alveolar space and carrying them to lymph nodes, where spores are released into the circulation via an unknown mechanism. However, studies by Cote et al. suggested that dissemination from the lung still occurs in macrophage-depleted mice (10, 11). In particular, mice depleted of alveolar macrophages were killed more readily by aerosol challenge with *B. anthracis* spores and had higher bacterial loads in the lungs than control mice (11). This finding suggested that the main role of macrophages during *B. anthracis* infections is bacterial clearance and that there is a macrophage-independent route of spore germination and dissemination. In addition, results from several groups indicated that both macrophage-like cell lines and primary macrophages are highly effective at killing newly germinated spores and vegetative bacilli (19, 20, 35). This *B. anthracis*-killing capability is probably also a characteristic of DCs, although there has not been a report describing studies investigating this topic.

We recently demonstrated that dormant spores of both the attenuated Sterne strain and the fully virulent Ames strain are capable of adherence to and internalization by lung epithelial cells. We also showed that in contrast to the findings with macrophages, internalized spores survive and perhaps germinate and replicate. Furthermore, spores traverse a barrier of lung epithelial cells from the apical to the basolateral side in the absence of phagocytes and without disrupting the barrier integrity (31). Taken together, the above-described observations provided a strong indication that the lung epithelium itself may play an important role in the spore dissemination process. However, direct evidence of in vivo spore uptake by epithelial cells of the lung has been lacking.

In this study, we undertook experiments to investigate the spatial distribution of *B. anthracis* spores soon after the delivery of spores into the lungs of wild-type (WT) BALB/c mice. A quantitative procedure was also developed to examine the adherence and internalization frequencies of the spores in vivo. The results provide clear in vivo evidence that the lung epi-

* Corresponding author. Mailing address: Center for Extracellular Matrix Biology, Institute of Biosciences and Technology, Texas A&M University Health Science Center, 2121 West Holcombe Blvd., Houston, TX 77030. Phone: (713) 677-7570. Fax: (713) 677-7576. E-mail: yxu@ibt.tamhsc.edu.

▽ Published ahead of print on 14 July 2008.

thelium is directly targeted by spores for adherence and internalization.

MATERIALS AND METHODS

Spore preparation. *B. anthracis* Sterne strain 7702 spores were prepared as stated previously (16, 31, 32).

Cell culture. MEF, a mouse embryonic fibroblast cell line (originally generated by Ruslan Medzhitov, Yale University), was provided by Dekai Zhang, Texas A&M Health Science Center-Institute of Biosciences and Technology (TAMHSC-IBT), Houston, TX. MLE15, a mouse lung epithelial cell line (originally generated by Jeffrey A. Whitsett, Cincinnati Children's Hospital), was provided by Scott E. Evans, University of Texas M. D. Anderson Cancer Center, Houston, TX. RAW264.7, a murine macrophage-like cell line, was purchased from the ATCC. Cells were maintained at 37°C in a humidified chamber with 5% CO_2 in Dulbecco's modified Eagle medium with 10% fetal bovine serum (FBS). All tissue culture reagents were purchased from Invitrogen.

Mouse infections. Six-week-old female BALB/c mice were used in the studies. Mice were maintained in a specific-pathogen-free environment in accordance with the National Institutes of Health (NIH) guidelines, and procedures were approved by the Institutional Animal Care and Use Committee at TAMHSC-IBT. Spores were injected into the mice through the trachea according to a procedure described previously (24). Briefly, mice were anesthetized by an intraperitoneal injection of 2,2,2-tribromoethanol (Sigma). An incision was made through the skin over the trachea, and the underlying tissue was separated to expose the trachea. A dosage of 25 μl of *B. anthracis* strain 7702 spores was injected into the trachea. The incision was then closed with wound clips (Roboz). The average inoculum was approximately 6×10^6 CFU/mouse.

Isolation of lung cells from spore-challenged mice and control mice. Two to 4 h post-spore inoculation, mice were anesthetized again and euthanized. The chest cavity was opened; the pulmonary vasculature was perfused with phosphate-buffered saline (PBS) through the right ventricle of the heart after the severing of the aorta. The lungs were lavaged two to three times with PBS containing 2.5 mM D-alanine.

To obtain crude lung cell suspensions (CLCS), we followed a procedure described previously (9), with modifications. Briefly, lungs were injected with ~1 ml of dispase (BD Biosciences) through the trachea and then removed from the chest and incubated in 2 to 3 ml of dispase solution containing 2.5 mM D-alanine for 1 h at room temperature to detach the cells from one another. Cells primarily from the lobes were then gently dispersed, and the cell suspension was filtered sequentially through 100-, 70-, and 40-μm-pore-size nylon cell strainers. The cells were then washed with PBS containing 2.5 mM D-alanine, yielding a CLCS. An aliquot of the suspension was used to calculate the number of cells by trypan blue exclusion in a hemacytometer. To determine the number of viable bacteria in the cell suspension, an aliquot of the cell suspension was lysed with 0.2% Triton X-100 and dilution plated. Another aliquot was lysed, heated at 65°C for 30 min, and plated to determine the number of heat-resistant dormant spores. The rest of the cells were fixed in 2% paraformaldehyde for 10 min at room temperature, washed, and stored at 4°C for further analysis by immunofluorescence staining.

For control experiments, lungs from uninfected healthy mice were lavaged two to three times with PBS and then injected with a dispase solution containing 2.5 mM D-alanine and amounts of strain 7702 spores comparable to the amounts of spores in the infection experiments described above. The lungs were then removed from the chest cavity and were processed in the same way as the lungs from spore-challenged mice.

Immunofluorescence staining of CLCS. Cells from the CLCS were allowed to attach to poly-L-lysine (Sigma)-coated coverslips during centrifugation at 200 × *g* for 5 min. The cells were blocked with PBS containing 10% FBS for 30 min at room temperature. To detect extracellular spores, the cells were incubated with rabbit antispore sera (custom rabbit polyclonal antibodies raised against formalin-killed *B. anthracis* spores; Strategic Biosolutions) at a 1:100 dilution in a solution of PBS and 2.5% FBS and were then incubated with goat anti-rabbit antibodies conjugated to Alexa Fluor 594 (1:250 dilution; Invitrogen). To detect intracellular spores, the cells were permeabilized with 100% methanol for 20 min at −20°C. The cells were blocked again and incubated with rabbit antispore antibodies (1:100), followed by goat anti-rabbit antibodies conjugated to Alexa Fluor 488 (1:250; Invitrogen). The cells were then incubated with a panepithelial mouse monoclonal antibody (clone C-11; Chemicon) recognizing cytokeratin (isoforms 4, 5, 6, 8, 10, 13, and 18), followed by goat anti-mouse antibodies conjugated to Alexa Fluor 350 (1:250; Invitrogen), to identify epithelial cells. To stain for CD11b- or CD11c-positive cells, cells were also incubated with biotin-labeled anti-mouse CD11b or CD11c antibodies (1:250 dilution; Invitrogen) and then with a streptavidin-Alexa Fluor 647 conjugate (1:250; Invitrogen). All incubations with antibodies were for 1 h at room temperature and were followed by three washes with PBS. Coverslips were mounted using Fluorsave (Calbiochem). Slides were viewed using a Zeiss Axiovert 135 microscope with a fluorescent light source. Images were recorded using an AxioCam MRc5 digital camera and were superimposed using the AxioVision software (Zeiss). At least 1,200 cells for each mouse in two independent experiments were counted to determine the percentage of cytokeratin-positive epithelial cells. At least 1,000 cytokeratin-positive epithelial cells for each mouse in two independent experiments were counted to determine the frequencies of spore adherence to and internalization by cytokeratin-positive cells. At least two independent investigators were responsible for the observation and counting of cells and spores. Student's *t* test was used for statistical analysis (with GraphPad software).

Immunfluorescence staining of cultured cell lines. To confirm the specificity of the anticytokeratin antibodies, MLE15, MEF, and RAW264.7 cells were grown on coverslips and fixed in 2% paraformaldehyde for 10 min at room temperature, permeabilized, blocked, and incubated with mouse anticytokeratin pan-monoclonal antibodies (1:100) followed by goat anti-mouse antibodies conjugated to Alexa Fluor 594 (1:250) according to the same procedure described above for the staining of lung cell suspensions. Nuclei were stained with 4′,6-diamidino-2-phenylindole (DAPI; 1:500). All camera exposure times were kept constant for accurate comparisons among cells from different cell lines when the AxioVision software was used to record images.

Determination of the labeling efficiency for spores. Spores were allowed to attach to poly-L-lysine (Sigma)-coated coverslips, fixed, and stained by the same procedure described above for the staining of spores in the lung cell suspensions. After the samples were mounted, the slides were viewed and ~1,000 spores were counted for each experiment. The results were reproduced at least four times.

Immunohistochemistry. Two and 4 h postinoculation, mice were anesthetized and euthanized. Lungs were collected, fixed in 10% formalin, dehydrated with a graded ethanol series and Citri Solv (Fisher Scientific), and embedded in paraffin. The lungs were sectioned into 3-μm slices and processed for hematoxylin and eosin (H&E) staining and immunofluorescence staining. Embedding, sectioning, and H&E staining were performed at the Breast Center Pathology Laboratory, Baylor College of Medicine, Houston, TX. Immunofluorescence staining was performed by first clearing the sections of paraffin by using a graded ethanol series and Citri Solv. The sections were permeabilized with 0.2% Triton X-100 for 5 min at room temperature and then incubated with 0.3 M glycine for 1 h. The sections were blocked with PBS containing 10% FBS for 30 min at room temperature. Spores were detected by incubation with rabbit antispore sera at a 1:100 dilution for 4 h at room temperature, followed by incubation with goat anti-rabbit antibodies conjugated to Alexa Fluor 594 (1:250) for 1 h. Cells were visualized by staining with phalloidin-Alexa Fluor 488 (1:200) and DAPI (1:500). All dilutions were made in PBS containing 2.5% FBS and 0.1% Triton X-100. Sections were viewed using the Zeiss Axiovert 135 fluorescence microscope and the camera system described above. Sections were also viewed using an LSM 510 confocal laser scanning fluorescence microscope and LSM 4.0 software (Zeiss). *z*-stacking was used to determine the intracellular location of spores. The *xy*, *yz*, and *xz* planar combinations were visualized.

RESULTS

Analysis of lung sections from mice challenged with *B. anthracis* spores. Lungs were collected 2 and 4 h after mice were inoculated with *B. anthracis* Sterne strain 7702 spores. H&E-stained sections of lungs from spore-challenged mice did not reveal any pathology or signs of inflammation compared with sections from healthy mice (data not shown). The airway epithelia and the alveolar walls appeared to be intact. This finding was expected, as damage in the lung is thought to be caused by vegetative cells. Vegetative growth in the lung does not occur during these early hours of infection (11, 15, 23).

Thin sections of the lungs (3 μm) were further analyzed by immunofluorescence staining for the presence of spores. Spores were observed to be associated with the epithelium of the airway and the alveoli at both 2 h (Fig. 1A and B) and 4 h (Fig. 1C and D) postinoculation. The majority of spores were single spores that were not clustered and were distributed relatively evenly throughout the alveolar sacs in the upper and

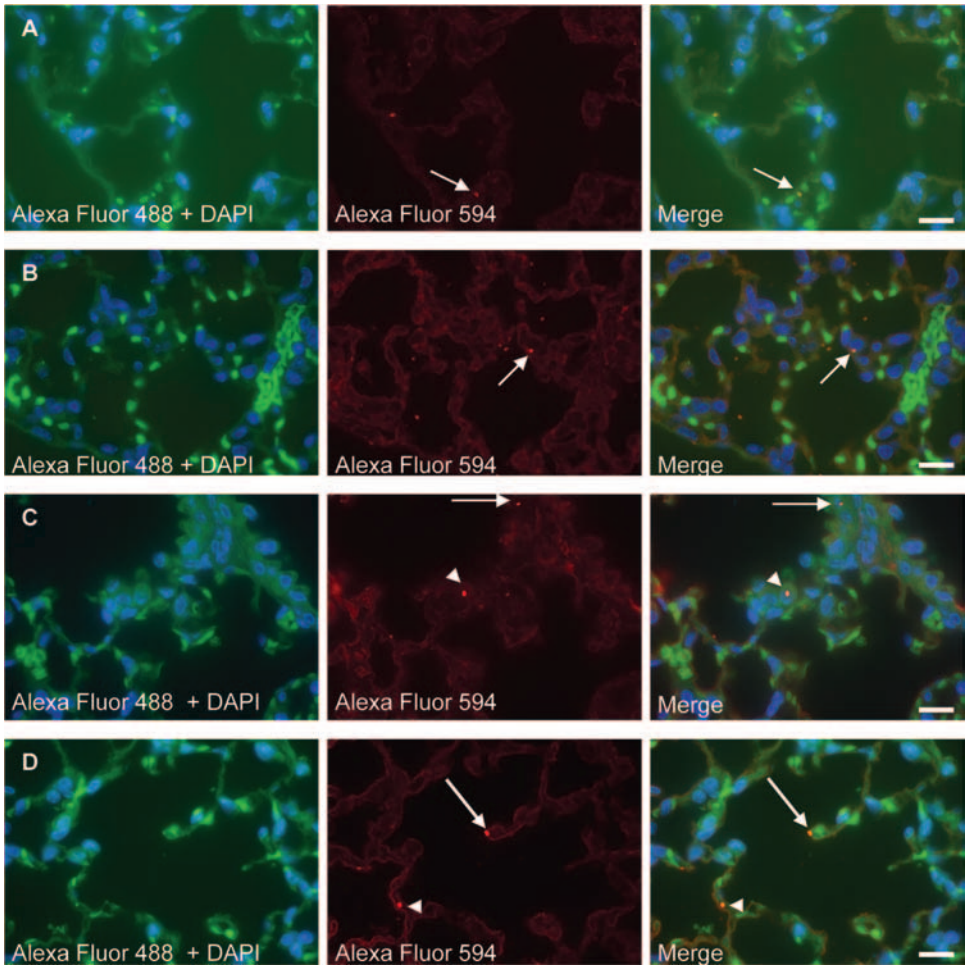

FIG. 1. Representative fluorescent microscopic images of lung sections from mice challenged with *B. anthracis* spores. Thin sections of lungs from mice inoculated with spores of *B. anthracis* Sterne strain 7702 were stained with rabbit antispore antibodies, followed by anti-rabbit antibodies conjugated to Alexa Fluor 549 (red), phalloidin-Alexa Fluor 488 (green), and DAPI (blue), as described in Materials and Methods. Superimposed images from the green and blue filters (corresponding to Alexa Fluor 488 and DAPI) are shown for the visualization of lung cells. Images from the red filter (corresponding to Alexa Fluor 594) are shown alone to reveal spores. (A and B) Lung sections obtained from mice 2 h postinfection. (C and D) Lung sections obtained from mice 4 h postinfection. Arrows and arrowheads indicate adhered spores and spores that appear to be on top of cells and may potentially be intracellular, respectively. Bars represent 10 μm.

lower lobes. Occasionally, nonadherent cells filled with multiple spores were seen in the alveolar spaces (data not shown). These cells may have been resident alveolar macrophages or recruited neutrophils that had not been removed by lavage. When comparing lung sections obtained from infected mice at the 2- and 4-h time points, we noticed that there tended to be more spores that were not associated with any lung cells in the 2-h samples, although we did not perform any quantitative measurement. This finding may reflect the possibility that some of these spores would have been phagocytosed between 2 and 4 h by macrophages. Another possibility is that the 4-h time point allowed more spores to reach epithelial surfaces and adhere to them.

We noticed that some of the spores that associated with the epithelium appeared to be on top of the cytoplasm or nuclei and might have been intracellular (e.g., Fig. 1C and D). In order to determine if any of them were intracellular, we used confocal laser scanning fluorescence microscopy to analyze lung sections obtained from infected mice 4 h postinoculation. Figure 2 is a representative confocal fluorescence microscopy image of a spore associated with the alveolar epithelium. Both the spore focus plane (Fig. 2A) and *z*-stacks (Fig. 2B) are shown. The *z*-stack projections clearly revealed that the spore was surrounded by F-actin, indicating the location of the spore to be intracellular. We analyzed 10 spores that were located on top of cells lining the alveoli. Eight of these were clearly intracellular. This result indicated that some of the spores associated with the epithelium were internalized.

Quantification of *B. anthracis* spore adherence to and internalization by epithelial cells of the lung in vivo. To further investigate spore adherence to and internalization by lung epithelial cells in vivo, we developed a procedure combining the method for isolating primary lung cells (9, 12, 13) with a differential immunofluorescence staining method that distinguished extracellular bacteria from intracellular ones (1).

In order to identify epithelial cells in the suspensions of lung

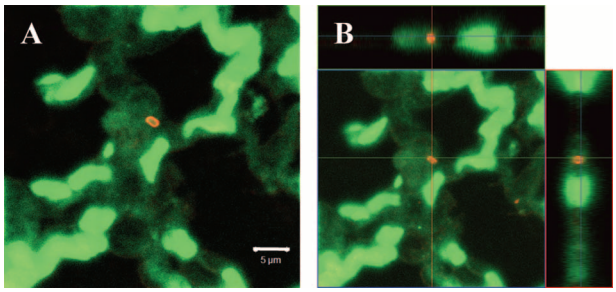

FIG. 2. Confocal laser scanning fluorescence microscopy images of a spore inside a cell lining an alveolus. Lung sections were obtained and stained as described in the legend to Fig. 1. F-actin was stained green, and spores were stained red. (A) Representative image of the spore focus plane. The bar represents 5 μm. (B) *z*-stack projections of the same image. The projections show all planar views, including *xy* (center panel), *xz* (right panel), and *yz* (top panel) stacks.

cells isolated from mouse lungs, a specific panepithelial antibody recognizing different cytokeratin isoforms (markers specific for epithelial cells) and, thus, different subtypes of epithelial cells was used. We first confirmed that the anticytokeratin antibody was specific for epithelial cells. The antibody was used to stain cells of MLE15, a mouse lung epithelial cell line; MEF, a mouse embryonic fibroblast cell line; and RAW264.7, a mouse macrophage-like cell line. Only the MLE15 cells stained positive with the anticytokeratin antibody (Fig. 3). We then used the antibody to stain cells from the CLCS. The numbers of cytokeratin-positive and -negative cells were determined using fluorescence microscopy. Approximately 19% of the cells in the CLCS were cytokeratin positive. To determine if the cytokeratin-positive cells were phagocytes that happened to be stained positive by the cytokeratin antibodies, cells from the CLCS were also stained with anti-CD11b or anti-CD11c antibodies. The results showed that cytokeratin-positive cells were not stained by anti-CD11b or anti-CD11c antibodies and that CD11b- or CD11c-positive cells were not stained by anticytokeratin antibodies (Fig. 4). Cells stained with secondary antibody controls exhibited only minimal background fluorescence (data not shown).

To detect extracellular and intracellular spores, a differential immunofluorescence staining method was used that resulted in extracellular spores' emitting red and green fluorescence and intracellular spores' emitting green fluorescence only. By this method, suspensions of lung cells obtained from infected mice at the 2- and 4-h time points were analyzed. Spores were observed to be adhered to and situated inside epithelial cells from the lungs of mice at both time points, suggesting that spore entry into lung epithelial cells was an early event during the course of infection. Examples of spores adhered to and located inside lung epithelial cells are shown in Fig. 5A to D. To determine if the green-only spores were green only due to their intracellular localization rather than to insufficient antibody staining, we stained spores with the relevant antibodies in the absence of lung cells. Of a total of approximately 4,000 spores examined in four independent staining experiments, all

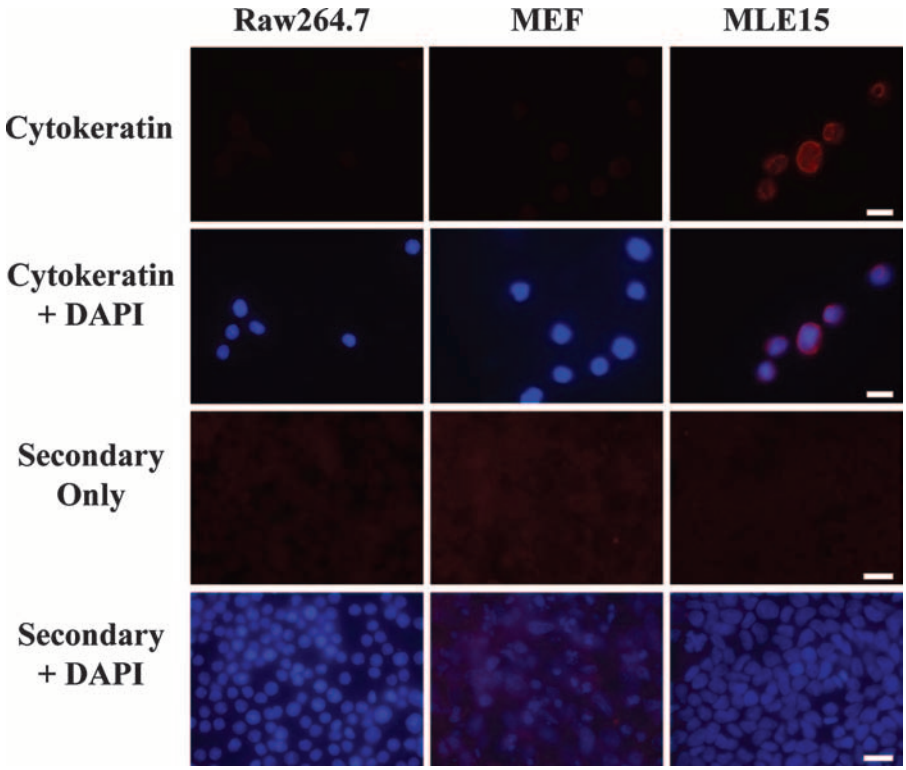

FIG. 3. The anticytokeratin antibodies are specific for epithelial cells. Mouse lung epithelial cells (MLE15), mouse embryonic fibroblasts (MEF), and mouse macrophage-like cells (RAW264.7) were fixed and stained with anticytokeratin antibody, followed by secondary antibodies conjugated to a red dye. DAPI was used to stain the nuclei as described in Materials and Methods. Only MLE15 cells stained positive by the anticytokeratin antibody. Controls with secondary antibody only showed minimal staining for all three cell lines. Bars represent 10 μm.

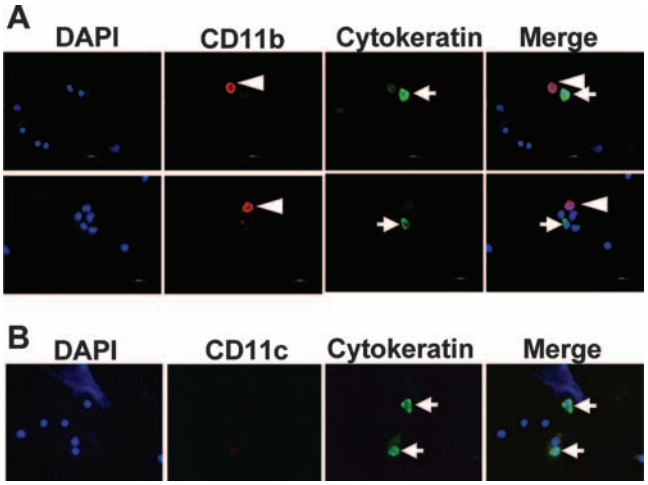

FIG. 4. Specific staining of epithelial cells isolated from the lungs of mice. CLCS from unchallenged mice were stained with antibodies against cytokeratin and CD11b (A) or CD11c (B) as described in Materials and Methods. DAPI (1:500) was used to stain the nuclei. Arrows indicate cytokeratin-positive cells, and arrowheads indicate CD11b-positive cells.

but 1 were stained both red and green, indicating that the antibody labeling was highly efficient. Representative images showing spores stained both red and green are presented in Fig. 5E to G. Thus, being green only was indicative of the intracellular localization of a spore.

The numbers of adhered and intracellular spores in the CLCS from mice infected for 4 h were recorded. The average ratios of adhered and intracellular spores relative to the number of epithelial cells were ~1.17% and ~0.62%, respectively (Fig. 6). The majority of the cells that had an adhered or intracellular spore had a cell-to-spore ratio of 1:1.

The germination status of *B. anthracis* in the CLCS from mice infected for 4 h was also determined. In order to accurately preserve the in vivo germination status of *B. anthracis*, D-alanine, a germination inhibitor (2, 25, 31, 32), was included (2.5 mM final concentration) in all the in vitro processing steps. Cells in the CLCS were lysed and either dilution plated directly for the determination of the total number of viable bacteria or heat treated before dilution plating for the analysis of heat-resistant dormant spores. On average, 93.8% of the bacteria in CLCS were heat resistant, indicating that most of them remained dormant at the 4-h time point. This finding was in agreement with those of previous studies (11, 15, 23).

The isolation of lung cells and the preparation of CLCS required several processing steps after the lungs were taken out of mice, i.e., incubation in the dispase solution for 1 h at room temperature, physical separation of lung cells, filtration through cell strainers, fixing of the cells, and washing of the cells by centrifugation and resuspension. In order to determine if spore adherence to and internalization by the cytokeratin-positive epithelial cells occurred in vivo rather than during these in vitro processing steps, control experiments were performed in parallel with the infection experiments. Lungs of

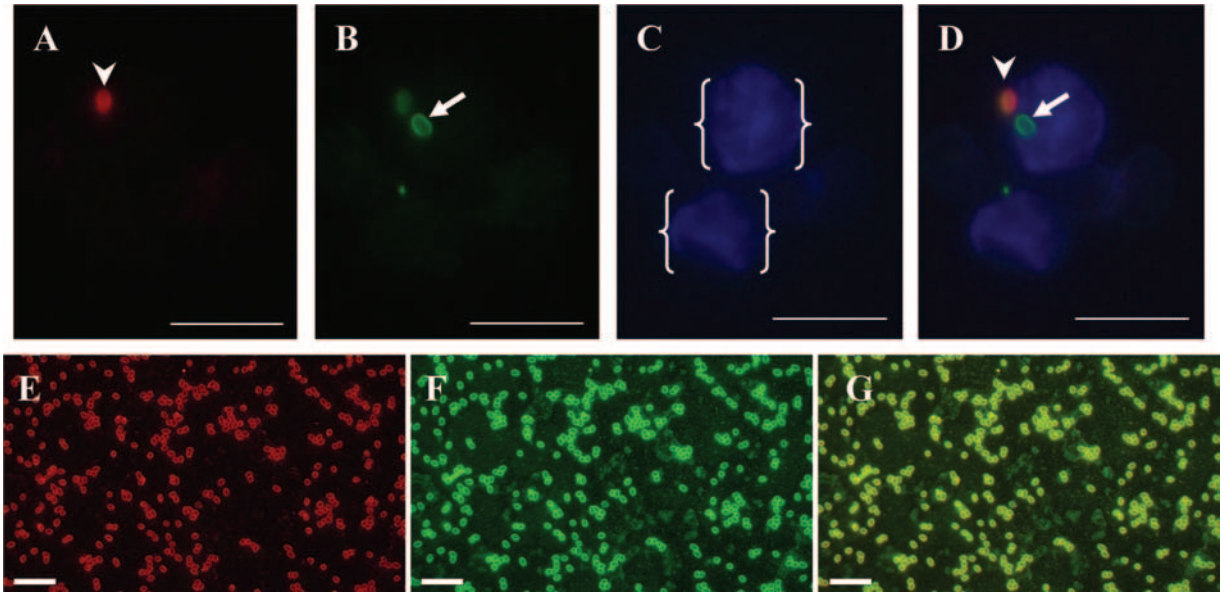

FIG. 5. Fluorescent microscopic images of extracellular adhered and intracellular spores in lung epithelial cells isolated from mice challenged with *B. anthracis* spores. (A to D) Staining of CLCS from mice infected for 4 h as described in Materials and Methods. (A) Nonpermeablized cells were stained with rabbit antispore antibodies, followed by a red secondary antibody for extracellular spores. (B) Permeabilized cells were stained with rabbit antispore antibodies, followed by a green secondary antibody for extracellular and intracellular spores. (C) Cells were stained with the anticytokeratin antibody, followed by a blue secondary antibody. The brackets outline two cytokeratin-positive epithelial cells. (D) A merged image showed that one of the cytokeratin-positive epithelial cells had an adhered spore (arrowhead) and an intracellular spore (arrow). (E to G) Staining of spores in the absence of cells to determine the spore staining efficiency. Spores were incubated with antispore antibodies, followed by anti-rabbit immunoglobulin G–Alexa Fluor 594 (E) and then anti-rabbit immunoglobulin G–Alexa Fluor 488 (F) according to the same procedure for staining spores in CLCS as described in Materials and Methods. A merged image showed that every spore was stained with both green and red fluorescent dyes (G). Bars represent 10 μm.

A

	Mice	Cfu†	%Intra/cell*	%Extra/cell*
4-hr infected Mice	1	7.2×10^6	1.04	2.27
	2	5.2×10^6	0.24	0.16
	3	3.2×10^6	0.68	1.91
	4	6.0×10^5	0.20	0.70
	5	5.6×10^5	0.23	0.35
	6	ND#	0.74	1.79
	7	ND#	1.22	1.02
Control Mice	1	1.1×10^6	0.00	0.00
	2	1.6×10^6	0.00	0.00
	3	1.1×10^6	0.00	0.00
	4	2.8×10^6	0.00	0.40
	5	2.2×10^6	0.09	0.64
	6	1.3×10^6	0.00	0.00
	7	5.0×10^5	0.00	0.00

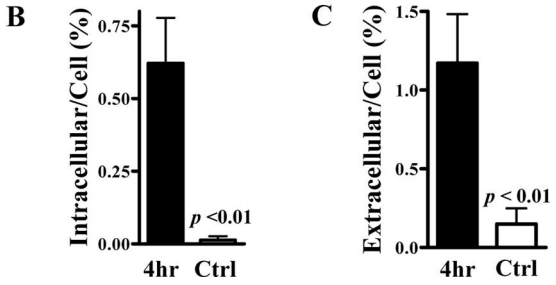

FIG. 6. Fluorescent microscopic quantification of intracellular and extracellular adhered spores in lung epithelial cells isolated from spore-challenged mice. CLCS from mice infected for 4 h or control mice were stained for the presence of adhered and intracellular spores and for cytokeratin-positive epithelial cells as described in the legend to Fig. 5. Approximately 1,000 cytokeratin-positive epithelial cells per mouse were examined. The results shown were combined from two independent experiments. (A) Results for each individual mouse. †, total counts of viable bacteria in the CLCS were determined by lysing an aliquot of the CLCS with Triton X-100 and performing dilution plating. *, percentages of intracellular spores (intra) and extracellular adhered spores (extra) relative to cytokeratin-positive epithelial cells were calculated as follows: total number of intracellular or extracellular adhered spores/total number of epithelial cells examined × 100. ND#, the viable bacterial counts were not determined. (B) Percentages of intracellular spores relative to cytokeratin-positive epithelial cells, expressed as the means ± the standard errors of the means (SEM; $n = 7$) for mice infected for 4 h and control mice. (C) Percentages of extracellular adhered spores relative to cytokeratin-positive epithelial cells, expressed as the means ± SEM ($n = 7$) for mice infected for 4 h and control mice. Statistical significance was calculated using Student's *t* test.

uninfected mice were harvested and processed exactly the same way as lungs from infected mice except that they were incubated in a dispase solution containing spores in amounts comparable to those used for infecting mice. We reasoned that if spore adherence and internalization occurred during the in vitro processing steps rather than in vivo, the staining of the CLCS from the control lungs, which had been incubated in spore-containing dispase, would reveal adhered and intracellular spores at frequencies comparable to those in samples from infected mice. However, we observed virtually no spore adherence or internalization in these control experiments (Fig. 6B and C) ($P = 0.002$ for comparison with results for mice infected for 4 h), indicating that the adherence and internalization frequencies we observed for the mice infected for 4 h resulted from in vivo events.

TABLE 1. Analysis of fluorescence microscopic quantification of *B. anthracis* spores in CLCS[a]

Parameter	Value
Total no. of cells in CLCS per mouse[b]	$1.7 \times 10^7 \pm 6 \times 10^5$
% of epithelial cells in CLCS[c]	19.13 ± 1.44
Total no. of epithelial cells in CLCS[d]	3.3×10^6
No. of intracellular spores per 100 epithelial cells[e]	0.62 ± 0.16
No. of extracellular adhered spores per 100 epithelial cells[e]	1.17 ± 0.31
Estimated no. of intracellular spores in total no. of epithelial cells in CLCS[f]	20,163
Estimated no. of adhered spores in total no. of epithelial cells in CLCS[f]	38,050

[a] Suspensions of lung cells obtained from mice 4 h postinfection were stained for the presence of adhered and intracellular spores and for cytokeratin-positive epithelial cells as described in Materials and Methods.
[b] The total number of cells in the CLCS per mouse is presented as the mean ± SEM ($n = 3$).
[c] The percentage of epithelial cells in the CLCS is presented as the mean ± SEM ($n = 4$) and was calculated as follows: number of cytokeratin-positive cells counted/total number of cells counted × 100.
[d] The total number of epithelial cells in the CLCS was calculated as follows: total number of cells in the CLCS per mouse × percentage of epithelial cells in the CLCS/100.
[e] The number of intracellular spores per 100 epithelial cells and the number of adhered spores per 100 epithelial cells are presented as the mean ± SEM ($n = 7$) of the results shown in Fig. 6.
[f] The number of intracellular or adhered spores in the total number of epithelial cells in the CLCS was calculated as follows: total number of epithelial cells in the CLCS × mean number of intracellular or adhered spores per 100 epithelial cells/100.

To gain a better idea of what our results meant for the animals, we estimated how many adhered and intracellular spores were in the lung epithelia by using the average frequencies, e.g., for every 100 lung epithelial cells, there were 1.17 adhered and 0.62 intracellular spores (Fig. 6 and Table 1). The total number of cells isolated from the lungs of mice was calculated to be approximately 17 million per mouse, of which ~19% were epithelial cells. Thus, these frequencies translated to approximately 38,050 spores adhered to and 20,163 spores inside lung epithelial cells per mouse at the 4-h time point (Table 1).

DISCUSSION

We present here in vivo evidence that *B. anthracis* spores were taken up by epithelial cells in the lung during early stages of infection. By fluorescence microscopy, spores were shown to be associated with the airway and alveolar epithelium 2 and 4 h after entering the lung. Confocal analysis revealed that some of the spores associated with the alveolar epithelium were surrounded by F-actin, indicating their intracellular localization. We further developed a procedure to confirm and determine in a quantitative manner that spores were taken up by lung epithelial cells in mice.

The impact of our findings with regard to *B. anthracis* pathogenesis is highly significant. Contrary to the conventional view that *B. anthracis* is a strictly extracellular pathogen, our findings clearly indicate an intracellular presence during pulmo-

nary anthrax. In recent years, many extracellular bacterial pathogens have been shown to possess the ability to invade different types of host nonphagocytic cells and act as opportunistic intracellular pathogens at various stages of infection. The invasion of host cells allows the pathogens to breach the various epithelial and endothelial barriers within the host, leading to more-disseminated infections and more severe clinical consequences. For example, *Streptococcus pneumoniae* has been shown previously to be able to breach the blood-brain barrier by trafficking through brain microvascular endothelial cells in a manner dependent on the platelet-activating factor receptor and pneumococcal choline-binding protein A (30). *Escherichia coli* K1 also invades brain microvascular endothelial cells to penetrate the blood-brain barrier in a process that involves the *E. coli* FimH adhesin and the putative host cell receptor CD48 (21) and intracellular Ca^{2+} signaling (22). The ability of *Neisseria gonorrhoeae* strains to invade epithelial cells at low phosphate levels is believed to be important during disseminating gonococcal infections. The invasion is mediated in a two-step process that involves first the binding of the *N. gonorrhoeae* outer membrane protein PorB serotype A to the human heat shock glycoprotein Gp96 and then the uptake of bacteria via the scavenger receptor SREC by epithelial cells (29).

We previously reported that *B. anthracis* spores are able to cross a barrier of lung epithelial cells without disrupting the barrier integrity, suggesting a transcellular trafficking route (31). Thus, the lung epithelium may be a direct portal for spores to breach the respiratory mucosal barrier. There is some evidence that InhA, a secreted metalloprotease of *B. anthracis*, is able to disrupt the integrity of an endothelial barrier but has no effect on epithelial cells (26). Therefore, once they escape from the epithelial cells, spores may potentially enter the pulmonary capillaries via a paracellular route. This scenario, however, does not exclude a potential role for alveolar macrophages and DCs in the dissemination process (8, 17, 18). Recent studies provided substantial evidence that *B. anthracis* is susceptible to phagocytic killing both in vitro and in vivo (10, 11, 19, 20, 35), suggesting that even though phagocytosis is highly efficient, dissemination via macrophages or DCs may be costly to *B. anthracis*. On the other hand, even though the frequency of spore uptake by epithelial cells is low compared to that by macrophages or DCs, spores inside epithelial cells are more likely to survive and grow, as we previously reported (31). It is possible that spores may hedge their bets by using a combination of these different portals to reach the circulation.

Previously, we demonstrated that spore germination is not required for uptake by epithelial cells, suggesting that surface components on dormant spores are sufficient to mediate spore adherence to and uptake by host cells (31). The outermost integument of a dormant spore is the exosporium, which consists of a hair-like nap made predominantly of the glycoprotein BclA and a basal layer of ~20 proteins. BclA was recently shown to mediate phagocytosis by macrophages in a Mac-1-dependent manner (28). Interestingly, in previous studies, spores of a *bclA* deletion mutant (Δ*bclA*) adhered to and were internalized by nonphagocytic cells dramatically better than WT spores (4, 28). We also observed approximately a 5- to 10-fold increase in the internalization of Δ*bclA* spores by polarized lung epithelial cells compared to that of WT spores (unpublished observation), suggesting that distinct mechanisms are involved in spore uptake by nonphagocytic cells (28). Investigation of the mechanisms for spore uptake is currently under way. Oliva et al. and Brahmhatt et al. showed the Δ*bclA* strain to be more virulent than the WT parent strain in animal models (5, 28), suggesting that there is a correlation between increased internalization by nonphagocytic cells and increased virulence and that internalization is an important aspect of the pathogenic process. However, other groups found no difference in virulence between WT and Δ*bclA* strains (3, 33). There are several possible explanations for the discrepancy, including the use of different bacterial and mouse strains, experimental methodologies, and spore dosages. The contribution of spore dosages may be of importance. An increase in virulence may not be readily revealed at high lethal dosages, as suggested by Oliva et al. (28).

The intracellular environment of nonphagocytic cells also provides a protective niche that facilitates bacterial colonization or persistence within the host. For example, uropathogenic *E. coli* was reported previously to establish quiescent intracellular reservoirs within the urinary bladder epithelium as a mechanism for persistence and a source for recurrent urinary tract infections (27). Group A streptococci appear to upregulate transforming growth factor β1 in infected hosts, leading to increased expression of the host cell receptor α5β1 integrin, resulting in enhanced host cell invasion and potentially persistence within the host (34). Anthrax infections can turn latent and become reactivated at a later time. Because of this risk, it is recommended that patients be treated with antibiotics for 60 days. Therefore, another implication of our results for *B. anthracis* pathogenesis may lie in this capacity for latency. Our findings may provide an explanation for the latent infections in that some spores may hide inside epithelial cells and be protected from the host immune responses.

Chakrabarty et al. recently reported that the lung epithelium actively participates in the innate immune response to *B. anthracis* spore exposure (7). Using a human lung slice model, the authors observed that exposure to spores resulted in the rapid activation of the mitogen-activated protein kinase signaling pathways extracellular signal-regulated kinase, p38, and Jun N-terminal protein kinase and the induction of several cytokines and chemokines, including interleukin-6, tumor necrosis factor alpha, interleukin-8, macrophage inflammatory protein 1α/β, and monocyte chemoattractant protein 1. Alveolar epithelial cells were shown to be one of the sources for the cytokines and chemokines. This finding alluded to another potential biological consequence of spore-epithelium interactions.

The average inoculum used in the studies described here was 6×10^6 CFU/mouse. This dosage was chosen based on results from preliminary studies in which different dosages were tested. A fourfold-higher dosage often resulted in animal death within minutes after injection, possibly due to airway blockage from the larger injection volume and/or the thicker suspension. Lower dosages yielded few or no intracellular spores within 1,000 epithelial cells, the typical number of epithelial cells counted per mouse. It is likely that if more cells had been counted, intracellular spores would have been found in those mice challenged with lower spore dosages. Fluorescence-activated cell sorting can sort a much larger number of cells; however, this method was not used because of the following concerns. We felt that a key issue in this study was to unam-

biguously identify intracellular and extracellular spores. By fluorescence microscopy, this identification could be achieved due to the distinctive morphology of spores, clearly separating them from any background fluorescence. Also, if a cell contained both an extracellular adhered spore and an intracellular spore, the intracellular spore would be missed by fluorescence-activated cell sorting because the red fluorescence emitted from the extracellular spore would be dominant. The quenching of extracellular fluorescence was not an option because the cells were permeabilized for cytokeratin staining.

The total number of cells isolated from the lungs of mice was calculated to be approximately 17 million per mouse. This result was in agreement with the data in a previous report, which used a similar lung cell isolation procedure (9). We found that approximately 19% of the cell population in the CLCS were cytokeratin-positive epithelial cells. Previous reports indicated that in rats, ~99% of the internal surface area of the lung is lined with alveolar type I (ATI) and ATII epithelial cells. These two types of cells constitute ~23 to 25% of total lung cells (9, 10). Assuming that the majority of lung epithelial cells were ATI and ATII cells, our percentage, albeit slightly smaller, was similar to those reported for rats.

We estimated that under our experimental conditions, there were approximately 38,050 spores adhered to and 20,163 spores situated inside the lung epithelial cells per mouse at the 4-h time point. Due to the concern for potential secondary infections which might complicate the interpretation of results, later time points were not included. It was reported previously that only a few organisms are required to cause infection in mice if *B. anthracis* is introduced directly into the bloodstream (50% lethal dose [LD_{50}], 6 to 25 spores) (24). Therefore, if even only a few of the spores inside epithelial cells escaped into the circulation, they would be sufficient to cause infection. Also, the number of spores inside epithelial cells accounted for ~0.3% of the average inoculum. The reported LD_{50} for BALB/c mice via intratracheal inoculation is in the order of $\sim 10^3$ spores (23, 24). Typically, dosages of 10 to 20 times the LD_{50} are used to cause 100% lethality. At these dosages, we would still expect to find some spores inside lung epithelial cells.

Previously, we presented in vitro data demonstrating that spores can be taken up by host epithelial cells (31). The internalization frequency we observed in vivo (~0.3% of total spores) was slightly lower than but still similar to our in vitro finding (~1% of total spores were taken up by primary small airway epithelial cells) (31). The in vivo adherence frequency (~0.6% of total spores), however, was much lower than our in vitro result (~25% of total spores). This difference may be due to two main reasons. One was that many of the extracellular spores were phagocytosed by macrophages and DCs in vivo. The other was that some extracellular adhered spores may have been detached during dispase treatment.

In our previous in vitro studies using cell cultures, spores were found to be taken up by cells of HT1080, a fibroblast cell line; Caco-2, an intestinal epithelial cell line; and A549, an ATII-like cell line, and by primary human small airway epithelial cells (31, 32). These results suggest that spores can be taken up by different cell types and epithelial cells of different tissue origins. Therefore, it is possible that spores can target different subsets of epithelial cells in the lung. On the other hand, the alveolar epithelium may play a big role as an escape portal due to its large surface area and proximity to the pulmonary capillaries.

Our procedure to quantify intracellular bacteria in vivo is novel and can be adapted to the study of host uptake of other bacterial pathogens. In order for us to conclude that the intracellular localization of the spores we observed was due to internalization events that occurred in vivo and not caused by any treatment during the in vitro processing steps, we set up two types of controls. First, we showed that the green-only staining of spores was due to their intracellular localization rather than insufficient labeling. Second, we demonstrated that there were virtually no spore adherence and internalization during the in vitro processing steps at our detection level.

In conclusion, we demonstrated that *B. anthracis* spores were taken up by lung epithelial cells in vivo during early stages of infection. This result indicated an intracellular presence during anthrax infections that has not been described previously and that may serve as a novel mechanism for spore dissemination and/or persistence in vivo. The findings bring an important new component, the lung epithelium, into the paradigm for pulmonary anthrax. Future studies to elucidate the mechanisms underlying spore internalization and trafficking across the epithelium and to understand the precise biological consequences of such an intracellular presence will be important. The procedure developed in this study can also be adapted to investigate the uptake of other bacterial pathogens in vivo and thus has general application.

ACKNOWLEDGMENTS

This work was supported by NIH grant AI061555 to Y. Xu and a career development award to Y. Xu through the Region VI Center for Biodefense and Emerging Infectious Diseases, funded by NIH grant U54 AI057156 (to D. Walker).

We thank Gabriela Bowden, Emanuel Smeds, and YaPing Ko, TAMHSC-IBT, for the care of mice; Magnus Höök, TAMHSC-IBT, Theresa M. Koehler, University of Texas Health Science Center, and Eric L. Brown, University of Texas School of Public Health, Houston, TX, for helpful discussions; Qiong Xue, TAMHSC-IBT, for technical assistance; Sufeng Mao and Zhongqiu Guo, Baylor College of Medicine, Houston, TX, for histology services; and Dekai Zhang, TAMHSC-IBT, and Scott Evans, University of Texas M. D. Anderson Cancer Center, Houston, TX, for providing cell lines.

REFERENCES

1. **Agerer, F., S. Waeckerle, and C. R. Hauck.** 2004. Microscopic quantification of bacterial invasion by a novel antibody-independent staining method. J. Microbiol. Methods **59:**23–32.
2. **Aronson, A.** 2002. Sporulation and delta-endotoxin synthesis by *Bacillus thuringiensis*. Cell. Mol. Life Sci. **59:**417–425.
3. **Bozue, J., C. K. Cote, K. L. Moody, and S. L. Welkos.** 2007. Fully virulent *Bacillus anthracis* does not require the immunodominant protein BclA for pathogenesis. Infect. Immun. **75:**508–511.
4. **Bozue, J., K. L. Moody, C. K. Cote, B. G. Stiles, A. M. Friedlander, S. L. Welkos, and M. L. Hale.** 2007. *Bacillus anthracis* spores of the *bclA* mutant exhibit increased adherence to epithelial cells, fibroblasts, and endothelial cells but not to macrophages. Infect. Immun. **75:**4498–4505.
5. **Brahmbhatt, T. N., B. K. Janes, E. S. Stibitz, S. C. Darnell, P. Sanz, S. B. Rasmussen, and A. D. O'Brien.** 2007. *Bacillus anthracis* exosporium protein BclA affects spore germination, interaction with extracellular matrix proteins, and hydrophobicity. Infect. Immun. **75:**5233–5239.
6. **Brittingham, K. C., G. Ruthel, R. G. Panchal, C. L. Fuller, W. J. Ribot, T. A. Hoover, H. A. Young, A. O. Anderson, and S. Bavari.** 2005. Dendritic cells endocytose *Bacillus anthracis* spores: implications for anthrax pathogenesis. J. Immunol. **174:**5545–5552.
7. **Chakrabarty, K., W. Wu, J. L. Booth, E. S. Duggan, N. N. Nagle, K. M. Coggeshall, and J. P. Metcalf.** 2007. Human lung innate immune response to *Bacillus anthracis* spore infection. Infect. Immun. **75:**3729–3738.

8. **Cleret, A., A. Quesnel-Hellmann, A. Vallon-Eberhard, B. Verrier, S. Jung, D. Vidal, J. Mathieu, and J. N. Tournier.** 2007. Lung dendritic cells rapidly mediate anthrax spore entry through the pulmonary route. J. Immunol. **178:**7994–8001.
9. **Corti, M., A. Brody, and J. Harrison.** 1996. Isolation and primary culture of murine alveolar type II cells. Am. J. Respir. Cell Mol. Biol. **14:**309–315.
10. **Cote, C. K., K. M. Rea, S. L. Norris, N. van Rooijen, and S. L. Welkos.** 2004. The use of a model of *in vivo* macrophage depletion to study the role of macrophages during infection with *Bacillus anthracis* spores. Microb. Pathog. **37:**169–175.
11. **Cote, C. K., N. Van Rooijen, and S. L. Welkos.** 2006. Roles of macrophages and neutrophils in the early host response to *Bacillus anthracis* spores in a mouse model of infection. Infect. Immun. **74:**469–480.
12. **Dahlin, K., E. M. Mager, L. Allen, Z. Tigue, L. Goodglick, M. Wadehra, and L. Dobbs.** 2004. Identification of genes differentially expressed in rat alveolar type I cells. Am. J. Respir. Cell Mol. Biol. **31:**309–316.
13. **Dobbs, L. G.** 1990. Isolation and culture of alveolar type II cells. Am. J. Physiol. **258:**L134–L147.
14. **Drysdale, M., S. Heninger, J. Hutt, Y. Chen, C. R. Lyons, and T. M. Koehler.** 2005. Capsule synthesis by *Bacillus anthracis* is required for dissemination in murine inhalation anthrax. EMBO J. **24:**221–227.
15. **Glomski, I. J., A. Piris-Gimenez, M. Huerre, M. Mock, and P. L. Goossens.** 2007. Primary involvement of pharynx and Peyer's patch in inhalational and intestinal anthrax. PLoS Pathog. **3:**e76.
16. **Green, B. D., L. Battisti, T. M. Koehler, C. B. Thorne, and B. E. Ivins.** 1985. Demonstration of a capsule plasmid in *Bacillus anthracis*. Infect. Immun. **49:**291–297.
17. **Guidi-Rontani, C.** 2002. The alveolar macrophage: the Trojan horse of *Bacillus anthracis*. Trends Microbiol. **10:**405–409.
18. **Guidi-Rontani, C., M. Weber-Levy, E. Labruyere, and M. Mock.** 1999. Germination of *Bacillus anthracis* spores within alveolar macrophages. Mol. Microbiol. **31:**9–17.
19. **Hu, H., Q. Sa, T. M. Koehler, A. I. Aronson, and D. Zhou.** 2006. Inactivation of *Bacillus anthracis* spores in murine primary macrophages. Cell. Microbiol. **8:**1634–1642.
20. **Kang, T. J., M. J. Fenton, M. A. Weiner, S. Hibbs, S. Basu, L. Baillie, and A. S. Cross.** 2005. Murine macrophages kill the vegetative form of *Bacillus anthracis*. Infect. Immun. **73:**7495–7501.
21. **Khan, N. A., Y. Kim, S. Shin, and K. S. Kim.** 2007. FimH-mediated *Escherichia coli* K1 invasion of human brain microvascular endothelial cells. Cell. Microbiol. **9:**169–178.
22. **Kim, Y. V., D. Pearce, and K. S. Kim.** 2008. Ca(2+)/calmodulin-dependent invasion of microvascular endothelial cells of human brain by *Escherichia coli* K1. Cell Tissue Res. **332:**427–433.
23. **Loving, C. L., M. Kennett, G. M. Lee, V. K. Grippe, and T. J. Merkel.** 2007. Murine aerosol challenge model of anthrax. Infect. Immun. **75:**2689–2698.
24. **Lyons, C. R., J. Lovchik, J. Hutt, M. F. Lipscomb, E. Wang, S. Heninger, L. Berliba, and K. Garrison.** 2004. Murine model of pulmonary anthrax: kinetics of dissemination, histopathology, and mouse strain susceptibility. Infect. Immun. **72:**4801–4809.
25. **McKevitt, M. T., K. M. Bryant, S. Shakir, J. L. Larabee, S. R. Blanke, J. Lovchik, C. R. Lyons, and J. D. Ballard.** 2007. Endogenous D-alanine synthesis and autoinhibition of *Bacillus anthracis* germination: effects on in vitro and in vivo infections. Infect. Immun. **75:**5726–5734.
26. **Mukherjee, D. V., M.-C. Chung, T. G. Popova, K. S. Kim, C. Bailey, and S. G. Popov.** 2007. Abstr. 107th Gen. Meet. Am. Soc. Microbiol., Toronto, ON, Canada, abstr. B-300.
27. **Mysorekar, I. U., and S. J. Hultgren.** 2006. Mechanisms of uropathogenic *Escherichia coli* persistence and eradication from the urinary tract. Proc. Natl. Acad. Sci. USA **103:**14170–14175.
28. **Oliva, C. R., M. K. Swiecki, C. E. Griguer, M. W. Lisanby, D. C. Bullard, C. L. Turnbough, Jr., and J. F. Kearney.** 2008. The integrin Mac-1 (CR3) mediates internalization and directs *Bacillus anthracis* spores into professional phagocytes. Proc. Natl. Acad. Sci. USA **105:**1261–1266.
29. **Rechner, C., C. Kühlewein, A. Müller, H. Schild, and T. Rudel.** 2007. Host glycoprotein Gp96 and scavenger receptor SREC interact with PorB of disseminating *Neisseria gonorrhoeae* in an epithelial invasion pathway. Cell Host Microbe **2:**393–403.
30. **Ring, A., J. N. Weiser, and E. I. Tuomanen.** 1998. Pneumococcal trafficking across the blood-brain barrier. Molecular analysis of a novel bidirectional pathway. J. Clin. Investig. **102:**347–360.
31. **Russell, B. H., R. Vasan, D. R. Keene, T. M. Koehler, and Y. Xu.** 2008. Potential dissemination of *Bacillus anthracis* utilizing human lung epithelial cells. Cell. Microbiol. **10:**945–967.
32. **Russell, B. H., R. Vasan, D. R. Keene, and Y. Xu.** 2007. *Bacillus anthracis* internalization by human fibroblasts and epithelial cells. Cell. Microbiol. **9:**1262–1274.
33. **Sylvestre, P., E. Couture-Tosi, and M. Mock.** 2002. A collagen-like surface glycoprotein is a structural component of the *Bacillus anthracis* exosporium. Mol. Microbiol. **45:**169–178.
34. **Wang, B., S. Li, P. J. Southern, and P. P. Cleary.** 2006. Streptococcal modulation of cellular invasion via TGF-β1 signaling. Proc. Natl. Acad. Sci. USA **103:**2380–2385.
35. **Welkos, S., A. Friedlander, S. Weeks, S. Little, and I. Mendelson.** 2002. In-vitro characterization of the phagocytosis and fate of anthrax spores in macrophage and the effects of anti-PA antibody. J. Med. Microbiol. **51:**821–831.

Editor: S. R. Blanke